Commun Nonlinear Sci Numer Simulat 17 (2012) 4690–4699

Contents lists available at ScienceDirect

Commun Nonlinear Sci Numer Simulat

journal homepage: www.elsevier.com/locate/cnsns

Dynamical analysis of turbulence in fusion plasmas and nonlinear waves ☆

R.L. Viana [a,*], S.R. Lopes [a], I.L. Caldas [b], J.D. Szezech [b], Z. Guimarães-Filho [c], G.Z. dos Santos Lima [d], P.P. Galuzio [a], A.M. Batista [e], Yu. Kuznetsov [b], I.C. Nascimento [b]

[a] Departamento de Física, Universidade Federal do Paraná, Caixa Postal 19044, 81531-990 Curitiba, Paraná, Brazil
[b] Instituto de Física, Universidade de São Paulo, 5315-970 São Paulo, Brazil
[c] International Institute for Fusion Science/PIIM, CNRS-Université de Provence, France
[d] Escola de Ciência e Tecnologia, Universidade Federal do Rio Grande do Norte, 59014-615 Natal, Rio Grande do Norte, Brazil
[e] Departamento de Matemática e Estatística, Universidade Estadual de Ponta Grossa, 84032-900 Ponta Grossa, PR, Brazil

ARTICLE INFO

Article history:
Available online 22 July 2011

Keywords:
Turbulence
Fluids
Plasmas
Nonlinear waves
Chaos
Tokamaks

ABSTRACT

Turbulence is one of the key problems of classical physics, and it has been the object of intense research in the last decades in a large spectrum of problems involving fluids, plasmas, and waves. In order to review some advances in theoretical and experimental investigations on turbulence a mini-symposium on this subject was organized in the Dynamics Days South America 2010 Conference. The main goal of this mini-symposium was to present recent developments in both fundamental aspects and dynamical analysis of turbulence in nonlinear waves and fusion plasmas. In this paper we present a summary of the works presented at this mini-symposium. Among the questions to be addressed were the onset and control of turbulence and spatio-temporal chaos.

1. Introduction

In a oft-quoted remark, Richard Feynman called turbulence the most important unsolved problem of classical physics [1]. In fact a great deal of work and effort have been put over the past decades into obtaining a comprehensive description of the onset and development of turbulence in fluids, plasmas and waves [2–4]. Fluid turbulence plays an important role in the time evolution of many systems ranging from the planetary and stellar atmospheres to the boundary layers on airplanes and cars. Plasma turbulence became increasingly important in magnetic fusion research, where turbulence at the plasma edge is believed to play a key role for the transport of energy and particles [5].

These wide ranging applications turns difficult to obtain a precise definition of the physical meaning of turbulence. A rough definition is that a turbulent flow is disordered in both space and time scales, but this is far from being a mathematical definition. Moreover, there is a huge difference between one-, two- and three-dimensional turbulent flows, between fully-developed turbulence (where a statistical analysis is acceptable) and weak turbulence (where coherent structures dominate the flow). Instead of a precise definition of turbulence, we cite two common traits of turbulent systems [6]: (i) a turbulent flow must be unpredictable, i.e. a small uncertainty at a given initial time will amplify so as to render impossible a precise deterministic prediction of its evolution; (ii) it should be able to mix transported quantities much more rapidly than if elementary processes (such as molecular diffusion in fluids) were involved.

☆ This work is dedicated to the memory of the late Professor Liu Kai (1931–2010), one of the pioneers of nonlinear studies in Brazil and an inspired teacher of generations of physicists.

* Corresponding author.
E-mail address: viana@fisica.ufpr.br (R.L. Viana).

1007-5704/$ - see front matter © 2011 Elsevier B.V. All rights reserved.
doi:10.1016/j.cnsns.2011.07.006

One of the paramount questions in turbulence research is the onset of turbulence, i.e. where is the transition from a laminar flow to a turbulent flow, a question already posed in the work of Osborne Reynolds, as far back as in 1883 [7]. The mechanism underlying the onset of turbulence received attention of outstanding physicists and mathematicians like Heisenberg [8], Landau [9] and Kolmogorov [10]. A fresh approach to this subject was given by Ruelle and Takens in a seminal paper on the role low-dimensional chaos plays in the onset of turbulence [11]. The question of the onset of turbulence has been recently studied by many authors [12–14].

Given the widespread interest in both the phenomenology and theoretical ideas in the description of turbulence in fluids, plasmas and waves, we proposed a mini-symposium in the Dynamics Days South America 2010 Conference on this general theme. We have received contributions on some aspects of experimental and computational research on turbulence in a variety of physically relevant systems. The goal of this paper is to summarize the works presented in this mini-symposium.

In the second section we present results of electrostatic turbulence in fusion plasmas experimentally obtained from discharges in the Brazilian Tokamak TCABR. The experimental results are used for estimating parameters of a three-wave model presenting mode conversion. A theoretical approach to the onset of wave turbulence is greated in Sections 3 and 4 to a system of three nonlinearly interacting and resonant waves and a forced drift wave, respectively. In both cases, the onset of turbulence is related to dynamical changes in a low-dimensional chaotic attractor of the system.

Besides the topics outlined above, the mini-symposium talk by Prof. Phil Morrison, entitled "The Hamiltonian and Action Principle Formulations of Continua," must be mentioned. Because the problem of turbulence is so difficult, many reduced models have been constructed and studied. If one removes the dissipation and driving terms from such models, then it was proffered in this talk that the resulting reduced model should be Hamiltonian. To this end a general discussion of Hamiltonian and action principle formulations of continua, e.g. fluid and plasma models, was given [15,16]. Two procedures were discussed for constructing such formulations for reduced models: a procedure based on Hamilton's principle of mechanics, adapted for continua [17,18], and a procedure based on Poisson brackets that embody the appropriate symmetries sought in a model and a choice of energy function. This amounts to a Lie algebra realization with an appropriate algebra of invariants in terms of the observables of the model. Transformations between the formulations obtained by the two procedures were described in general and the particular examples of ideal magnetohydrodynamics [19] and Braginskii's fluid model with gyroviscosity [20,21] were discussed. Because the first procedure has been documented in the publications cited, it will not be further described here. The second procedure will be published elsewhere.

2. Electrostatic turbulence in the TCABR tokamak

Tokamaks are toroidal systems of magnetic confinement of plasmas, and are promising candidates to be the core of a future nuclear fusion reactor [22]. The usefulness of the tokamak as a fusion reactor relies, however, on its capability to maintain a sufficiently hot plasma during a time interval large enough to yield energy conversion. One of the factors conspiring against this ultimate goal is the loss of energy and particles through transport processes not yet fully understood, notwithstanding controlled. Electrostatic turbulence is the main cause of the anomalous particle and energy transport at the tokamak plasma edge [23]. Many experimental results suggest that electrostatic turbulence can be driven by Mirnov oscillations [24,25]. In particular, this influence has been observed in the Brazilian tokamak TCABR (Tokamak Chauffage Alfvén Brésilien), where the turbulent spectrum of the floating potential at the plasma edge has been observed to be affected by a magnetic mode created by an ergodic magnetic limiter [26–28].

In the TCABR the magnetic and electrostatic frequency spectra present a peculiar partial superposition, thus enhancing coupling, normally small, between these two kinds of fluctuations. Moreover, in some TCABR regimes the MHD activity increases at different instants of time during the discharge, and reaches high amplitudes with a narrow wave-number spectrum and a well-defined peak on the Mirnov frequency ($\sim$13 kHz) [29–31,31]. During this high MHD activity the electrostatic turbulence synchronizes with the MHD activity at the Mirnov frequency and its broadband wave-number spectra is greatly modified [31].

The hydrogen circular plasma of the TCABR tokamak has major radius $R = 61$ cm and minor radius $a = 18$ cm, with a maximum plasma current of 100 kA, with duration 100 ms, and toroidal magnetic field $B_0 = 1.1$ T. At the plasma edge the electron plasma density is $n_e \approx 3 \times 10^{18}$ m^{-3}, and the electron temperature is $T_e \approx 10$ eV [29]. The floating potential has been measured in the plasma edge and scrape-off layer regions ($0.9 < r/a < 1.2$) by a set of movable Langmuir probes. Magnetic fluctuations were measured by Mirnov coils located at $r/a = 1.08$.

In order to illustrate the coupling between magnetic and electrostatic oscillations we show in Fig. 1(a) the spectrogram of floating potential fluctuations, where the oscillation frequencies (in kHz) are plotted against the discharge duration, the corresponding power spectral densities $S_{\phi\phi}$ being plotted in a color scale. In Fig. 1(b) we depict the corresponding spectrogram for Mirnov oscillations, where the periods of magnetic activity are associated with peaks of the power spectral density S_{BB}. It is clearly seen a spontaneous increase of electrostatic activity following an increase in the magnetic activity, starting just before 40 ms with a dominant frequency of $\sim$13 kHz which extends up to 60 ms, with at least two overtones corresponding to higher harmonics of the dominant frequency. This clearly indicates a coupling between electrostatic and magnetic fluctuations and, moreover, a frequency synchronization between them.

In Fig. 1(c) and (d) we show the time series of the floating potential (normalized by its standard deviation) for two time intervals where the MHD activity is low and high, respectively. Comparing these series with the corresponding data for the

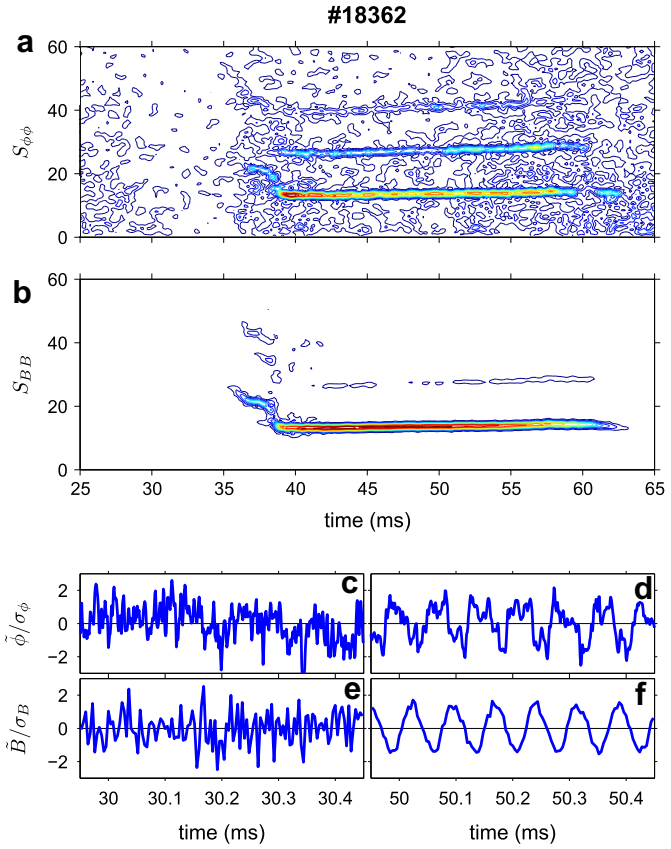

Fig. 1. Spectral fluctuation data obtained in the TCABR tokamak (shot 18362) with an electrostatic probe located at $r = 17.0$ cm. (a) Spectrogram of electrostatic potential fluctuations; (b) Spectrogram of Mirnov oscillations; (c) and (d) are normalized floating potential fluctuations at different time intervals; (e) and (f) are the corresponding normalized Mirnov oscillations.

magnetic (Mirnov) fluctuations, depicted in Fig. 1(e) and (f), respectively, we observe that, after the intense MHD activity sets in, the Mirnov oscillations are almost sinusoidal, with a well defined frequency of ~13 kHz, the corresponding potential fluctuations having a strong harmonic content at that frequency. The strong distortion in the latter signal corresponds to the overtones observed in the spectrogram of Fig. 1(a).

A standard way to detect and quantify mode coupling is the use of bicoherence, which is well-suited to deal with nonlinear wave couplings through triplets, using higher-order statistics [32–34]. The bispectrum is the Fourier transform of the third-order cumulant-generating function. Let $\phi(f)$ be the Fourier transform of the time signal at the mode frequency f. The bicoherence is defined as [34]

$$b^2(f_1,f_2) = \frac{|\langle \phi(f_1)\phi(f_2)\phi^*(f_3)\rangle|^2}{\langle|\phi(f_1)\phi(f_2)|^2\rangle\langle|\phi(f_3)|^2\rangle}, \tag{1}$$

such that $f_3 = f_1 + f_2$, and measures of the amount of nonlinear coupling between the modes $\phi(f_i)$ in a wave triplet with frequencies f_1, f_2, and f_3 satisfying the resonance condition $f_3 = f_1 + f_2$. If the three modes are phase-coupled, there follows that $b^2(f_1,f_2)$ is nearly the unity; whereas it is almost zero if the modes are barely or no coupled at all. In Fig. 2(a) and (b) we plot the summed bicoherence for the floating potential without and with magnetic (Mirnov) oscillations $S_{\phi\phi\phi}(f) = \sum' b^2(f_1,f_2)$, where the primed sum means that the summation is performed over all frequencies such that $f = f_1, f_2$, or $f_1 + f_2$. It is clearly seen that the second case indeed represents a mode coupling between fluctuations involving the 13 kHz mode.

Since the bicoherence results indicate a coupling between electrostatic and magnetic oscillations as a nonlinear triplet interaction, we modelled this situation by using a three-wave model with quadratic nonlinearities [30]

$$\frac{d\phi_1}{dt} + i\omega_1\phi_1 = \Lambda^1_{2,3}\phi_2^*\phi_3^* + \gamma_1\phi_1, \tag{2}$$

$$\frac{d\phi_2}{dt} + i\omega_2\phi_2 = \Lambda^2_{3,1}\phi_3^*\phi_1^* + \gamma_2\phi_2, \tag{3}$$

$$\frac{d\phi_3}{dt} + i\omega_3\phi_3 = \Lambda^3_{1,2}\phi_1^*\phi_2^* + \gamma_3\phi_3, \tag{4}$$

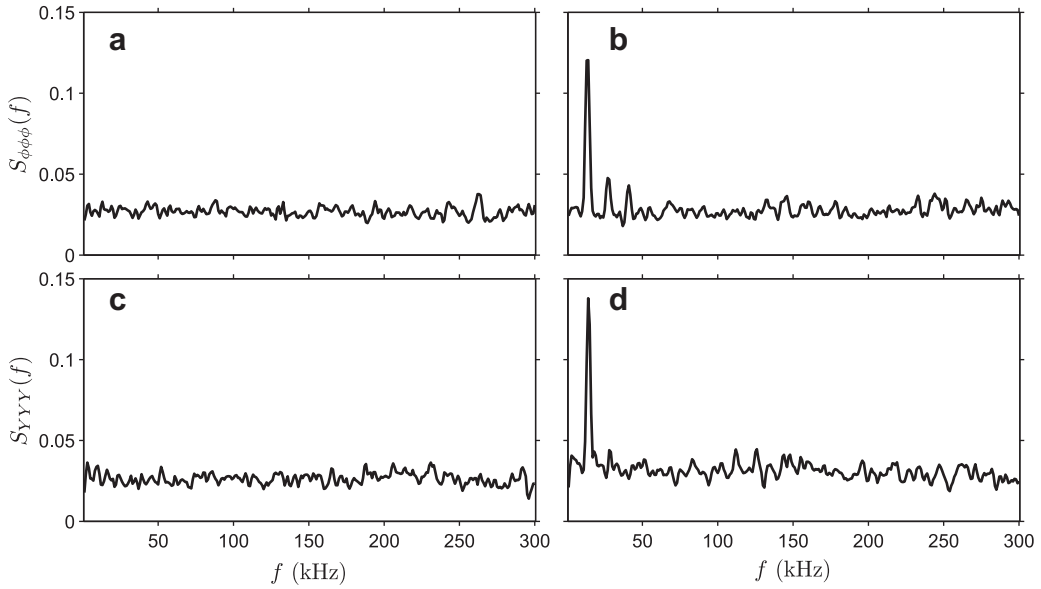

Fig. 2. (a) and (b): summed bicoherence for the floating potential fluctuations measured in TCABR, corresponding to the time series depicted in Fig. 1(c) and (d), respectively. (c) and (d): summed bicoherence for a theoretical model of three-wave coupling.

where $\phi_j = \phi_{\mathbf{k}_j}$ and $\omega_j = \omega_{\mathbf{k}_j}$ are the amplitudes and frequencies of three modes retained in a pseudo-spectral decomposition of the Hasegawa–Mima equation, satisfying the following resonant conditions $\mathbf{k}_1 + \mathbf{k}_2 + \mathbf{k}_3 = \mathbf{0}$ and $\omega_{\mathbf{k}_1} + \omega_{\mathbf{k}_2} + \omega_{\mathbf{k}_3} \approx 0$. We model the effect of the Mirnov oscillations by a driving term $\exp(\pm i\Omega t)$, where Ω is the dominant Mirnov oscillations frequency, added to the three-mode Eqs. (2)–(4). We also included an incoherent noise in order to mimic the stochastic content present in the electrostatic oscillations measured in TCABR [30].

In the numerical simulations using Eqs. (2)–(4) with driving and noise, we used parameter values compatible with the edge region of the tokamak TCABR. The electron temperature was taken to be $T_e = 10$ eV; and the density gradient is $|\nabla n_0|/n_o = 5\ \mathrm{m}^{-1}$, from which we estimated the ion cyclotron frequency to be 1.05×10^8 Hz and the length scale is thus $\rho_s \approx 10^{-3}$ m. We estimated the coupling coefficients in Eqs. (2)–(4) as $\Lambda^1_{2,3} = -1.15 \times 10^{-2}, \Lambda^2_{3,1} = 5.30 \times 10^{-3}$, and $\Lambda^3_{1,2} = 6.00 \times 10^{-4}$. Moreover, the time-periodic driving term representing the influence of magnetic oscillations has a normalized frequency $\Omega = 9.0 \times 10^{-4}$. In Fig. 2(c) and (d) we show the summed bicoherence of the variable standing for the electrostatic potential in our theoretical model, without and with magnetic coupling, and the results are both qualitatively and quantitatively similar to the experimental ones.

3. Onset of turbulence in a three-wave model

One of the paradigm models in wave turbulence is the resonant nonlinear three-wave interaction model, where the complex amplitudes A_α, $\alpha = 1, 2, 3$, describe three dispersive monochromatic waves propagating along the x-direction [36,40–43]. Their wave numbers and frequencies satisfy matching conditions for the triplet: $\mathbf{k}_3 = \mathbf{k}_1 + \mathbf{k}_2$ and $\Omega_{\mathbf{k}_3} = \Omega_{\mathbf{k}_1} - \Omega_{\mathbf{k}_2} - \delta$, where δ is a small frequency mismatch. Each wave has a constant group velocity $v_{g\alpha} = d\Omega_{\mathbf{k}_\alpha}/dk_\alpha$, given by its linear dispersion relation, and we assume that $v_{g2} > v_{g1} > v_{g3}$. This describes a scenario where $A_1(x,t)$ is the parent wave amplitude, $A_2(x,t)$ and $A_3(x,t)$ being the faster and slower daughter waves, respectively [35]. For example, in non-magnetized plasmas A_1 can be a transverse electromagnetic wave, A_2 an ion-acoustic wave, and A_3 is a Langmuir wave (anti-Stokes mode) [36].

If the nonlinearities present in the wave interactions are sufficiently weak, only quadratic terms in the wave amplitudes need to be considered. The resulting model is thus [37]

$$\frac{\partial A_1}{\partial t} + v_{g1}\frac{\partial A_1}{\partial x} = A_2 A_3 + v_1 A_1 + D\frac{\partial^2 A_1}{\partial x^2}, \tag{5}$$

$$\frac{\partial A_2}{\partial t} + v_{g2}\frac{\partial A_2}{\partial x} = -A_1 A_3^* + v_2 A_2, \tag{6}$$

$$\frac{\partial A_3}{\partial t} + v_{g3}\frac{\partial A_3}{\partial x} = i\delta A_3 - A_1 A_2^* + v_3 A_3, \tag{7}$$

where D is a diffusion coefficient, and we add growth and decay rates by the coefficients $v_1 > 0$ and $v_{2,3} < 0$, which represent energy injection (through wave 1) and dissipation (through waves 2 and 3), respectively.

In the following we will choose parameters as $v_{g1} = 0.0$, $v_{g2} = 1.0$, $v_{g3} = -1.0$, $\delta = 0.1$, and $D = 1.0$, and the rates v_α, $\alpha = 1, 2, 3$, are the parameters to be varied. We integrate Eqs. (5)–(7) using a pseudo-spectral method using a fixed number N of modes in Fourier space (for a one-dimensional box of length L with periodic boundary conditions) [38]

$$A_\alpha(x,t) = \sum_{n=-(N/2)+1}^{N/2} |a_{\alpha,n}(t)| \exp\left\{i[\kappa_{\alpha,n}x + \phi_{\alpha,n}(t)]\right\}, \quad (\alpha = 1,2,3), \tag{8}$$

where $a_{\alpha,n}(t)$ is the time-dependent Fourier coefficient corresponding to the mode number $\kappa_{\alpha,n} = 2\pi n/L$, and whose evolution is governed by a system of $6N$ coupled ordinary differential equations, since the mode amplitudes themselves are complex variables. We used a box length $L = 2\pi/\kappa_{1,1} = 2\pi/0.89$. The initial conditions are chosen as $F_{1,0}(0) = 0.500 + i0.000$, and $F_{2,\pm1}(0) = 0.001 + i0.001$, where $F_{\alpha,n}(t) = a_{\alpha,n}(t) \exp(i\phi_{\alpha,n}(t))$, all the other modes being set to zero.

A representative set of results is depicted in Fig. 3, where spatio-temporal plots are drawn for different dynamical regimes observed, and in the third axis we plotted the real daughter wave amplitude $|A_2|$ using a color code. In Fig. 3(a) the show a flat profile in real space evolving periodically in time characterizing a spatially homogeneous state with non-chaotic dynamics. The modes with $\kappa_{\alpha,0} \neq 0$ and $\kappa_{\alpha,i} = 0$, $(i \neq 0)$, correspond to such a spatially homogeneous state. It turns out that the spatially homogeneous states lie on a 3-dimensional invariant subspace $\mathcal{M}$ of the full phase space of the system. This homogeneous manifold is invariant in the sense that, once an initial condition is placed there, the ensuing trajectory remains in $\mathcal{M}$ for all further times under the dynamics generated by the $\kappa_{\alpha,0}$ modes. Accordingly, the spatially inhomogeneous modes $\kappa_{\alpha,n}$ are related to directions transversal to $\mathcal{M}$. When the dissipation is increased, the dynamics of the homogeneous state becomes chaotic ([Fig. 3(b)]) and, for a further increase spatial modes eventually become excited ([Fig. 3(c)]). As a consequence the wave energy is distributed along temporal and spatial modes, provoking inhomogeneous spatial patterns.

In order to characterize quantitatively the loss of transversal stability of the homogeneous manifold and the ensuing excitation of spatial modes we resort to the Kuramoto complex order parameter [39]

$$z_\alpha(t) = R_\alpha(t)\exp(i\Phi_\alpha(t)) \equiv \frac{1}{N}\sum_{n=-(N/2)+1}^{N/2} \exp(i\varphi_{\alpha,n}(t)), \tag{9}$$

where $R_\alpha(t)$ and $\Phi_\alpha(t)$, $\alpha = 1, 2, 3$, are the amplitude and angle, respectively, of a centroid phase vector for a one-dimensional lattice of Fourier modes with periodic boundary conditions. The phase angle is computed as

$$\varphi_{\alpha,n}(t) = \arctan\left\{\frac{\mathrm{Im}[A_{\alpha,n}(t)]}{\mathrm{Re}[A_{\alpha,n}(t)]}\right\}. \tag{10}$$

We compute the order parameter magnitude average $\overline{R_\alpha} = \lim_{T\to\infty}\frac{1}{T}\int_{n=0}^{T} R_\alpha(t)dt$, such that a spatially homogeneous state is characterized by $\overline{R_\alpha} = 1$, since there occurs a coherent superposition of the phase vectors with the same amplitude at each time for all discrete positions in the reciprocal lattice. The lower is the value of $\overline{R_\alpha}$, the less the spatial coherence of the system state. Accordingly the breakdown of the totally coherent state is a criterion for the appearance of spatial modes, what follows the loss of transversal stability of the homogeneous manifold.

It is necessary that the dynamics in the homogeneous manifold be chaotic in order to provide a pump mechanism to feed energy to the spatial modes. This can be seen in Fig. 4(a), where we plot the bifurcation diagram for $|A_1(1,t)|$ and in Fig. 4(b) the average order parameter for the parent wave $\overline{R_1}$ as a function of the decay rate of the daughter waves $v_{2,3}$. Within the numerical accuracy the spatially homogeneous state is transversely stable for values of the decay rate higher than $v_{CR} \approx -1.96$, which is the value for which $\overline{R_1}$ ceases to be equal to the unity. The (purely temporal) dynamics in the homogeneous manifold can be either periodic or chaotic, as shown by Fig. 4(a): it starts as a period-1 orbit for small values of $|v_{2,3}|$

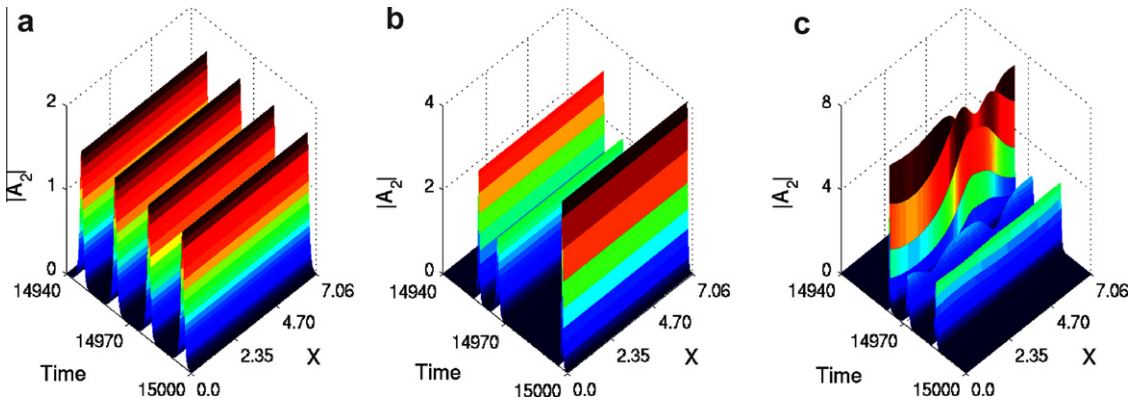

Fig. 3. Space–time plots of the real wave amplitude $|A_2|$ (also indicated by a color scale) when (a) $v_1 = 0.1$, $v_{2,3} = -1.0$; (b) $v_1 = 0.1$, $v_{2,3} = -1.6$; (c) $v_1 = 0.5$, $v_{2,3} = -4.0$.

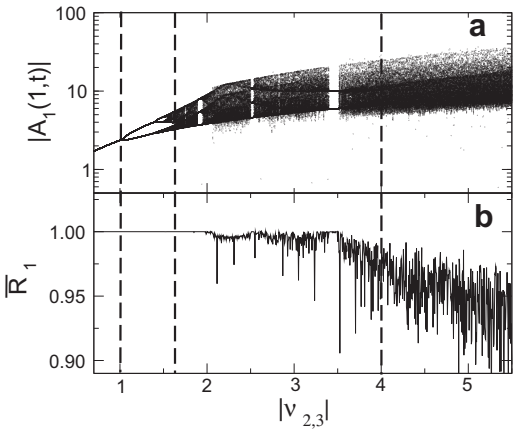

Fig. 4. (a) Bifurcation diagram for $|A_1(1,t)|$ as a function of the decay rate $|\nu_{2,3}|$. We denote by dashed lines three particular parameter values which correspond to the cases from Fig. 3(a), (b) and (c). (b) Time-averaged order parameter for parent wave versus decay rate for $T = 210^5$, after 10^4 transient iterations.

and undergoes a period-doubling cascade to chaotic bands which disappear due to a crisis and are followed by a period-3 window. The loss of transversal stability of the homogeneous manifold occurs just after a three-band chaotic attractor suffers an internal crisis and merge into a single large chaotic orbit at ν_{CR}.

4. Onset of turbulence in a forced drift-wave model

As a representative example of a spatially extended dynamical system with two solution branches we consider the damped and forced drift wave equation [44,45]

$$\phi_t + a\phi_{txx} + c\phi_x + f\phi\phi_x + \gamma\phi = -\epsilon\sin(Kx - \Omega t), \tag{11}$$

For magnetically confined fusion plasmas $\phi(x,t)$ is the non-dimensional electric potential of a drift wave propagating along the poloidal direction of a toroidal plasma, where the constants a, c, and f stand for plasma and wave parameters, and we introduced a phenomenological linear damping term with coefficient γ [46]. The effect of other possibly relevant modes is represented by a time-periodic driving with amplitude ϵ, wave number K and frequency Ω.

Eq. (11), for certain parameters values, displays a transition from pure temporal chaos without spatial mode excitation to spatio-temporal chaos. This transition has been described in Refs. [47,45] as resulting from an interior crisis, whereby a chaotic attractor collides with a high-dimensional chaotic saddle. However, the intermittent behavior that follows from an interior crisis turns to be different from that observed in the numerical simulations. We found that the solutions wander in an intermittent fashion between two *non-overlapping* states of distinct wave energies, whereas an interior crisis would yield an intermittent alternation between overlapping states: one of which is the pre-critical attractor "ghost", and the other is the post-critical attractor made available by the crisis. Since these states are non-overlapping, we propose that the observed behavior is due not to an interior crisis but rather due to two-state on–off intermittency.

Since the x-coordinate is either an angle or can be a bounded variable, we suppose a Fourier expansion

$$\phi(x,t) = \sum_{n=0}^{N} |\varphi_n(t)| e^{i\kappa_n x}, \tag{12}$$

where $\phi_k(t)$ are time-dependent amplitudes and $\kappa_n \equiv 2\pi n/L$ in a box of length $L = 2\pi$ and periodic boundary conditions. Notice that the mode $\kappa_0 = 0$ is purely temporal, whereas $\kappa_\alpha = \alpha = 1,2,3,\ldots$ stand for the spatial modes. On substituting (12) into (11), one obtains a system of N coupled ordinary differential equations, solved using a 12rd order Adams predictor–corrector scheme. In the numerical simulations to be reported in this letter we used $N = 128$ modes, unless stated otherwise, and we kept fixed the following parameters [46]: $a = -0.28711$, $c = 1.0$, $f = -6.0$, $\gamma = 0.1$, $K = 1.0$, and $\Omega = 0.65$, such that ϵ will be our control parameter. The initial conditions for the system of N coupled mode equations are $\varphi(0) = 0.01$, $\varphi_1(0) = \varphi_2(0) = \sigma_1 R(0,1)$, $\varphi_n(0) = \sigma_2\ R(0,1)$, for $n \geqslant 3$, where $\sigma_1 = 0.001$, $\sigma_2 = 10^{-5}$, and $R(0,1)$ is a pseudo-random number chosen within the interval $[0,1]$ with uniform probability. We stress that these initial conditions are different from those used in Ref. [46], where a solitary-wave-solution of the unperturbed case ($\epsilon = 0, \gamma = 0$) was chosen.

The possible solutions of the initial and boundary value problem defined by Eq. (11) can be best characterized by computing the wave energy, defined as

$$E(t) = \frac{1}{2\pi}\int_0^{2\pi} \frac{1}{2}\left[\phi^2(x,t) - a\phi_x^2(x,t)\right]dx, \tag{13}$$

which turns to be an integral of motion for the unperturbed case. For the parameter values explored in this work the wave dynamics is chaotic, but even so the energy difference is bounded [48,47].

As the parameter ϵ is increased from zero, we have a steady state energy difference $\Delta E = E(t) - E(0)$ with a few peaks, and asymptoting to a value about 0.05, until a first bifurcation value $\epsilon_\ell = 0.19955$ is achieved [49]. For $\epsilon_\ell < \epsilon < \epsilon_h = 0.20100$ we have alternation of energy values between two values, the former $\sim$0.05 lower branch and a $\sim$0.25 higher branch. Finally, for $\epsilon > \epsilon_h$ the energy fluctuates about the higher branch value, never to return to the lower branch. The lower and upper branches of the wave energy are two energy states for which, when $\epsilon_\ell < \epsilon < \epsilon_h$, there is intermittent behavior. These two states can be represented, in the Fourier mode space, by different energy hypersurfaces we call A and B. For $\epsilon < \epsilon_\ell$ the state A is stable with respect to transversal displacements from the energy hypersurface, whereas B is transversely unstable and not reached by typical initial conditions.

Since a few temporal modes are excited in the state A, it corresponds to temporal chaos combined with regular (periodic) spatial patterns. This is illustrated by the space–time plot depicted in Fig. 5(a), obtained for $\epsilon < \epsilon_\ell$, which displays a chaotic time evolution with regular spatial behavior akin to a travelling wave solution. However, as the state B becomes transversely stable, a large number of spatial modes are excited. A rather extreme example, considering $\epsilon > \epsilon_h$, is shown in Fig. 5(b), for which we see aperiodic behavior in both spatial and temporal scales (spatio-temporal chaos). For a small interval of time (*ca.* 25 pseudo-periods) some travelling waves, which appear due to the inductor term, are continuously created and destroyed.

In order to provide a quantitative characterization of the dynamics in space and time we can resort to Lyapunov exponent computation in Fourier space. In this case, each Fourier mode in the discrete transform (12) can be considered a degree of freedom, and the corresponding Lyapunov exponent is computed for the set of N wave amplitude equations $\varphi_n(t)$, with $n = 0, 1, 2, \ldots N$. The exponent related to $n = 0$ corresponds to the temporal dynamics, whereas the $n \geqslant 1$ case stands for spatial degrees of freedom and can be used to detect spatial mode excitation [37].

Accordingly, in Fig. 6 we plot the time evolution of the 30 first Lyapunov exponents out of $N = 128$ modes corresponding to the wave amplitudes in Eq. (12). The black and red curves stand for longitudinal and maximal transversal exponent, respectively. When a given exponent decays with time as a power-law, it is considered zero when time tends to infinity; and, if this decay is faster than a power law, the exponent goes to negative values. In the case $\epsilon = 0.195 < \epsilon_\ell$, only the Lyapunov exponent related to the time ($n = 0$) asymptotes to a nonzero value [Fig. 6(a)], confirming our claim that only temporal chaos is observed. The exponents corresponding to spatial modes are shown to decay in a roughly power-law ($n = 1$) and even faster rates (for $n \geqslant 2$). Hence those spatial modes, if excited at all, can have at most periodic behavior (and a possible

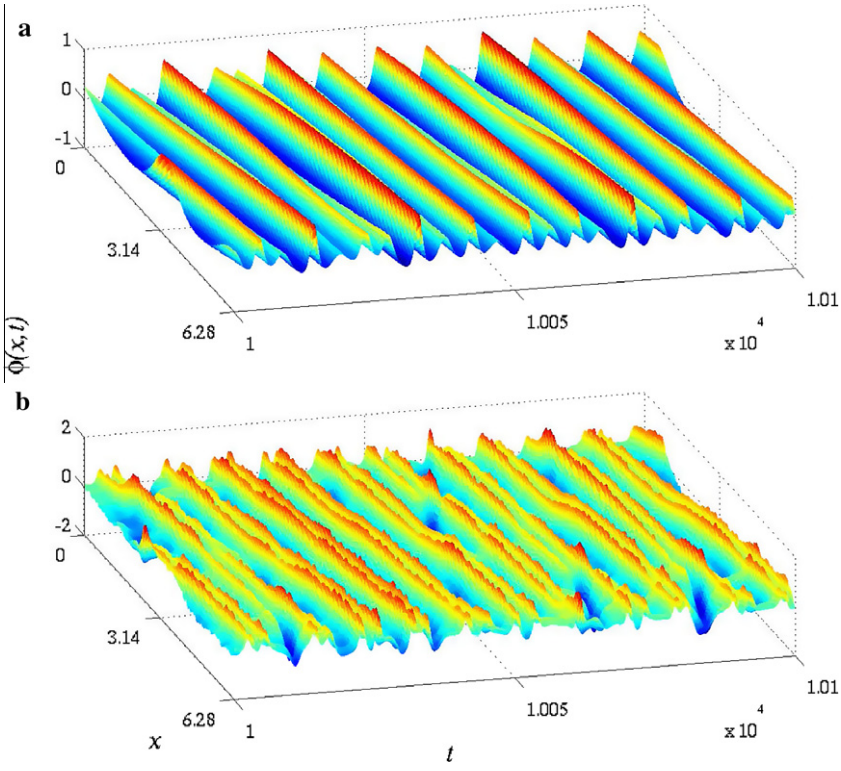

Fig. 5. Space–time plots for the wave amplitude for (a) $\epsilon = 0.1990 < \epsilon_\ell$; (b) $\epsilon = 0.2100 > \epsilon_h$.

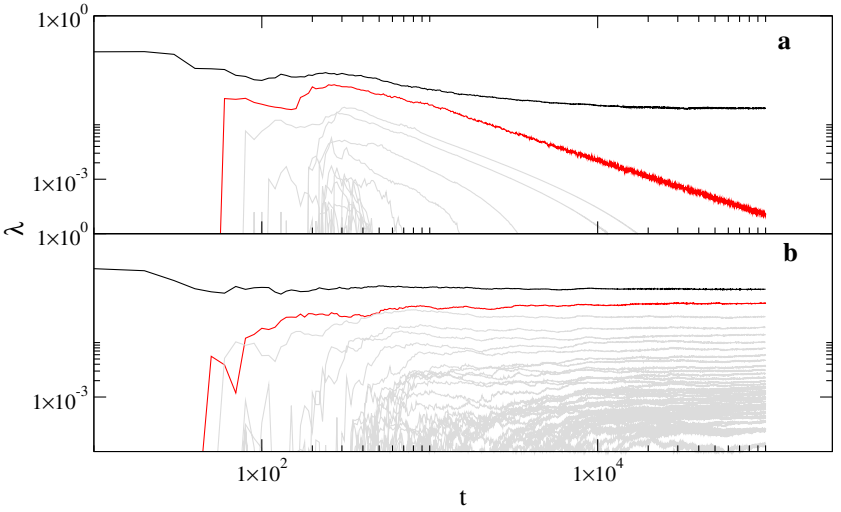

Fig. 6. The 30 largest Lyapunov exponents corresponding to modes in Fourier space for (a) $\epsilon = 0.195$; (b) $\epsilon = 0.205$.

quasiperiodic one). By way of contrast, for $\epsilon > \epsilon_h$ a large number of the exponents for $n \neq 0$ do not vanish, hence many spatial modes become chaotic [Fig. 6(b)]. This spatial mode excitation involving so many Fourier modes suggests the existence of a strongly turbulent state.

5. Conclusions

In this paper we collected works presented at the mini-symposium on turbulence in fluids and plasmas, a part of the Dynamics Days South America 2010 Conference, held in São José dos Campos, Brazil. The main focus of this symposium was to show recent experimental and theoretical advances in turbulence occurring in waves and plasmas. The symposium was opened by the lecture of Prof. Morrison on how one can use Hamiltonian and action principle methods to obtain fluid and plasma models for the study of turbulence.

The work presented by I. L. Caldas (Section 2) dealt with the data analysis of experimental observation of coupling in the electrostatic turbulence observed in TCABR tokamak plasma discharges with high MHD activity. The coupling was identified through bispectral analysis involving electrostatic fluctuations driven by the MHD fluctuations. This phenomenon was also modelled by a chaotic dynamical system based on three coherent nonlinearly coupled drift modes with incoherent noise and a time-periodic driving at the MHD frequency. The inclusion of incoherent noise was used to reproduce both the linear and nonlinear spectral characteristics of turbulence data without high MHD activity. The external time-periodic driving term was introduced to reproduce spectral features observed during high MHD activity. The results of this model, using bicoherence analysis, agree with the experimental observations.

The paper presented by R. L. Viana (Section 3) proposed a scenario for explaining the onset of spatio-temporal chaos in spatially extended systems by the nonlinear excitation of spatial modes powered by the chaotic dynamics in a low-dimensional and spatially homogeneous attractor. In mathematical terms, there must be an invariant subspace (embedded in the system phase space) containing a chaotic attractor with pure temporal chaos, i.e. no spatial modes. Energy is pumped from this chaotic state to excite inhomogeneous spatial modes. The onset of wave turbulence, or spatio-temporal chaos, occurs when some unstable periodic orbit, embedded in the spatially homogeneous chaotic attractor, loses transversal stability (with respect to the homogeneous subspace). The energy formerly confined in the temporally chaotic dynamics of the homogeneous state is thus imparted to the spatial modes excited after the loss of transversal stability.

The contribution presented by S. R. Lopes (Section 4) revealed the existence of two-state on–off intermittent behavior in the damped and forced drift wave equation. The two states with respect to which the system oscillates are stationary solutions corresponding to different wave energies. In the language of (Fourier mode) phase space these states are embedded in two invariant manifolds that become transversely unstable in the regime where two-state on–off intermittency sets in. The distribution of laminar duration sizes is compatible with the similar phenomenon occurring in time only in the presence of noise, as shown by the corresponding scaling laws, which present two regimes: a power-law scaling for small plateaus and an exponential (fat) tails for large plateaus. In spatially extended systems like this the noisy effect is provided by the spatial modes excited by the perturbation. We show that this intermittency is a precursor of the onset of strong turbulence in the system.

Acknowledgments

This work was made possible by partial financial support of FAPESP, CNPq, CAPES, Fundação Araucárias, and RNF-CNEN (Brazilian Fusion Network).

References

[1] Falkovich G, Sreenivasan KR. Lessons from hydrodynamic turbulence. Phys Today 2006;59:43–9.
[2] Batchelor GK. The theory of homogeneous turbulence. Cambridge: Cambridge University Press; 1953.
[3] Frisch U. Turbulence: The legacy of A.N. Kolmogorov. Cambridge: Cambridge University Press; 1995.
[4] Bohr T, Jensen MH, Paladin G, Vulpiani A. Dynamical systems approach to turbulence. Cambridge: Cambridge University Press; 1998.
[5] Günter S. Focus on turbulence in magnetized plasmas. New J Phys 2002;4:1. doi:10.1088/1367-2630/4/1/001.
[6] Lesieur M. Turbulence in Fluids. Dordrecht: Martinues Nijhoff; 1987.
[7] Reynolds O. An experimental investigation of the circumstances which determine whether the motion of water shall be direct or sinuous, and of the law of resistance in parallel channels. Philos Trans R Soc 1883;174:935–82. The collected works of Reynolds are freely available for download at <http://www.archive.org/details/papersonmechanic01reynrich>.
[8] Heisenberg W. Zur statistischen Theorie der Turbulenz. Z Phys 1948;124:628–57.
[9] Landau LD, Lifshitz EM. Fluid Mechanics. 2nd. ed. New York: Pergamon Press; 1987.
[10] Kolmogorov A.N., The local structure of turbulence in incompressible viscous fluid for very large Reynolds number, Dokl. Akad. Nauk USSR, 30 (4) (1941) (in Russian). An English translation is available in Proc R Soc Lond A 434 (1991) 9-13.
[11] Ruelle D, Takens F. On the nature of turbulence. Commun Math Phys 1971;20:167–92.
[12] Waleffe F. On a self-sustaining process in shear flows. Phys Fluids 1997;9:883–900.
[13] Waleffe F, Wang J. Transition threshold and the self-sustaining process. In: Mullin T, Kerswell R, editors. IUTAM Symposium on Laminar-Turbulent Transition and Finite-Amplitude Solutions. Springer; 2005. p. 85–106.
[14] Eckhardt B. Turbulence transition in pipe flow: some open questions. Nonlinearity 2008;21:T1–9.
[15] Morrison PJ. Poisson brackets for fluids and plasmas. In: Tabor M, Treve Y, editors. Mathematical Methods in Hydrodynamics and Integrability in Dynamical Systems, American Institute of Physics Conference Proceedings, 88. New York: American Institute of Physics; 1982. p. 13–46.
[16] Morrison PJ. On hamiltonian and action principle formulations of plasma dynamics. In: Eliasson B, Shukla P, editors. New Developments in Nonlinear Plasma Physics, Proceedings for the 2009 ICTP College on Plasma Physics, American Institute of Physics Conference Proceedings, 1188. New York: American Institute of Physics; 2009. p. 329–44.
[17] Morrison PJ. Hamiltonian description of the ideal fluid. Rev Mod Phys 1998;70:467–521.
[18] Morrison PJ. Hamiltonian and action principle formulations of plasma physics. Phys Plasmas 2005;12:058102.
[19] Morrison PJ, Greene JM. Noncanonical Hamiltonian density formulation of hydrodynamics and ideal magnetohydrodynamics. Phys Rev Lett 1980;45:790–4. 48 (1982) 569-573.
[20] Morrison PJ, Caldas IL, Tasso H. Hamiltonian formulation of two-dimensional gyroviscous MHD. Z Naturforsch 1984;39a:1023–7.
[21] Tassi E, Chandre C, Morrison PJ. Hamiltonian derivation of the Charney–Hasegawa–Mima equation. Phys Plasmas 2009;16:082301.
[22] Horton W. Drift waves and transport. Rev Mod Phys 1999;71:735–78.
[23] Hidalgo C., Alejaldre C., Alonso A., Alonso J., Almoguera L., de Aragón F., Ascasíbar E., Baciero A., Balbín R., Blanco E., Botija J., Brañas B., Calderón E., Cappa A., Carmona J.A., Carrasco R., Castejón F., Cepero J.R., Chmyga A.A., Doncel J., Dreval N.B., Eguilior S., Eliseev L., Estrada T., Ferreira J.A., Fernández A., Fontdecaba J.M., Fuentes C., García A., García-Cortés I., Gonçalves B., Guasp J., Herranz J., Hidalgo A., Jiménez R., Jiménez J.A., Jiménez-Rey D., Kirpitchev I., Khrebtov S.M., Komarov A.D., Kozachok A.S., Krupnik L., Lapayese F., Liniers M., López-Bruna D., López-Fraguas A., López-Rázola J., López-Sánchez A., de la Luna E., Marcon G., Martín R., McCarthy K.J., Medina F., Medrano M., Melnikov A.V., Mendez P., van Milligen B., Nedzelskiy I.S., Ochando M., Orozco O., de Pablos J.L., Pacios L., Pastor I., Pedrosa M.A., de la Peña A., Pereira A., Petrov A., Petrov S., Portas A., Rapisarda D., Rodríguez-Rodrigo L., Rodríguez-Solano E., Romero J., Salas A., Sánchez E., Sánchez J., Sánchez M., Sarksian K., Silva C., Schchepetov S., Skvortsova N., Tabarés F., Tafalla D., Tolkachev A., Tribaldos V., Vargas I., Vega J., Wolfers G., Zurro B., Overview of TJ-II experiments, Nucl. Fusion 45 (2005) S266-S275.
[24] Heller MVAP, Castro RM, Brasílio ZA, Caldas IL, da Silva RP. Edge turbulence spectrum alterations driven by resonant fields. Nucl Fusion 1995;35:59–67.
[25] Devynck P, Bonhomme G, Martines E, Stöckel J, Van Oost G, Voitsekhovitch I, et al. Spatially resolved characterization of electrostatic fluctuations in the scrape-off layer of the CASTOR tokamak. Plasma Phys Contr Fusion 2005;47:269–80.
[26] Evans TE, Goniche M, Grosman A, Guilhem D, Hess W, Vallet J-C. Magnetic perturbation effects on boundary plasmas during high power lower hybrid current drive in Tore Supra. J Nucl Mater 1992;196–198:421–5.
[27] Ghendrih Ph., Baucoulet M., Colas L., Grosman A., Guirlet R., Gunn J., Loarer T., Azaroual A., Basiuk V., Beaumont B., Baucoulet A., Beyer P., Bramond S., Bucalossi J., Capes H., Corre Y., Costanzo L., De Michelis C., Devynck P., Faron S., Friant C., Garbet X., Giannella R., Grisolia C., Hess W., Hogan J., Ladurelle L., Laugier F., Martin G., Mattioli M., Meslin B., Monier-Garbet P., Moulin D., Nguyen F., Pascal J.-Y., PecquetA.-L., Pagouria B., Reichle R., Saint-Laurent F., Vallet J.-C., Zabiago M., and the TORE SUPRA Team, Progress in ergodic divertor operation on Tore-Supra, Nucl Fusion 42 (2002) 1221-1250. .
[28] Heller MVAP, Caldas IL, Ferreira AA, Saettone EAO, Vannucci A. Tokamak turbulence at the scrape-off layer in TCABR with ergodic magnetic limiter. J Plasma Phys 2007;73:295–306.
[29] Nascimento IC, Kuznetsov YuK, Guimarães-Filho ZO, El Chamaa-Neto I, Usuriaga O, Fonseca AMM, et al. Suppression and excitation of MHD activity with an electrically polarized electrodes at the TCABR tokamak plasma edge. Nucl Fusion 2007;47:1570–6.
[30] dos Santos Lima GZ, Guimarães-Filho ZO, Caldas IL, Nascimento IC, Kuznetsov YuK, Batista AM, et al. Bicoherence in electrostatic turbulence driven by high magnetohydrodynamic activity in Tokamak Chauffage Alfvén Brésilien. Phys Plasmas 2009;19:042508.
[31] Guimarães-Filho ZO, Caldas IL, Viana RL, Heller MVAP, Nascimento IC, Kuznetsov YuK, et al. Electrostatic turbulence driven by high MHD activity in TCABR tokamak. Phys Plasmas 2008;15:062501.
[32] Ritz ChP, Powers EJ, Bengtson RD. Experimental measurement of three-wave coupling and energy cascading. Phys Fluids B 1989;1:153–63.
[33] van Milligen BPh, Hidalgo C, Sánchez E, Pedrosa MA, Balbín R, García-Cortés I, et al. Statistically robust linear and nonlinear wavelet analysis applied to plasma edge turbulence. Rev Sci Instrum 1997;68:967–70.
[34] Ferreira AA, Heller MVAP, Caldas IL. Experimental analysis of mode coupling and plasma turbulence. Phys Plasmas 2000;7:3567–72.
[35] Kaup DJ, Reiman A, Bers A. Space-time evolution of nonlinear three-wave interactions. Rev Mod Phys 1979;51:275–309.
[36] Chian AC-L, Lopes SR, Alves MV. Generation of auroral whistler-mode radiation via nonlinear coupling of Langmuir waves and Alfvén waves. Astron Astrophys 1994;290:L13–L16;;
Chian AC-L, Rizzato FB. J Plas Phys 1994;51.
[37] Szezech Jr JD, Lopes SR, Viana RL, Caldas IL. Physica D. Bubbling transition to spatial mode excitation in an extended dynamical system 2009;238:516–25;
Szezech Jr JD, Lopes SR, Caldas IL, Viana RL. Blowout bifurcation and spatial mode excitation in the bubbling transition to turbulence. Physica A 2011;390:365–73.
[38] Szezech Jr JD, Lopes SR, Viana RL. Onset of spatiotemporal chaos in a nonlinear system. Phys Rev E 2007;75:67202.
[39] Kuramoto Y. Chemical Oscillations, Waves, and Turbulence. Berlin: Springer Verlag; 1984.
[40] Turner L. Driving-dissipative Euler's equations for a rigid body: a chaotic system relevant to fluid dynamcis. Phys Rev E 1996;54:5822–5825;;
Li YC. Chaos in wave interactions. Int J Bifurcat Chaos 2007;17:85–98.
[41] Rundquist A, Durfee III CG, Chang Z, Herne C, Backus S, Murnane MM, et al. Phase-matched generation of coherent soft x-rays. Science 1998;280:1412–5;
Stegeman GI, Segev M. Optical spatial solitons and there interactions: universality and diversity. Science 1999;286:1518–23;
Picozzi A, Haeltermann M. Parametric three-wave soliton generated from incoherent light. Phys Rev Lett 2001;86:2010–3.
[42] Chow CC, Bers A, Ram AK. Spatiotemporal chaos in the nonlinear three-wave interaction. Phys Rev Lett 1992;68:3379–82.

[43] Lopes SR, Rizzato FB. Nonintegrable dynamics of the triplet-triplet spatiotemporal interaction. Phys Rev E 1999;60:5375–84.
[44] Horton W. Nonlinear drift waves and transport in magnetized plasma. Phys Rep 1990;192:1–177.
[45] Rempel EL, Chian AC-L. Origin of transient and intermittent dynamics in spatiotemporal chaotic systems. Phys Rev Lett 2007;98:014101.
[46] He K, Salat A. Hysteresis and onset of chaos in periodically driven nonlinear drift waves. Plasma Phys Contr Fusion 1989;31:123–41.
[47] He K. Riddling of the orbit in a high-dimensional torus and intermittent energy bursts in a nonlinear wave system. Phys Rev Lett 2005;94:034101.
[48] He K, Chian AC-L. On-off collective imperfect phase synchronization and bursts in wave energy in a turbulent state. Phys Rev Lett 2003;91:034102; Rempel EL, Chian AC-L, Macau EEN, Rosa R. Analysis of chaotic saddles in high-dimensional dynamical systems: the Kuramoto-Sivashinsky equation. Chaos 2004;14:545–56.
[49] Galuzio PP, Lopes SR, Viana RL. Two-state on-off intermittency and the onset of turbulence in a spatiotemporally chaotic system. Phys Rev Lett 2010;105:055001.